Enhanced carbon nanotubes dispersion in epoxy matrices using a CNT tailored block copolymer

J.F. Guedes *, M. Martins, N. Rocha *

INEGI – Institute of Science and Innovation in Mechanical and Industrial Engineering, Campus da FEUP, Rua Dr. Roberto Frias, 400, Porto 4200-465, Portugal

Abstract

Carbon nanotubes (CNT) have been extensively studied, and special attention has been given to their introduction in epoxy matrices, for further reinforcement of carbon fibre reinforced composites. However, the obtained improvements are highly dependent on the level of CNT dispersion and distribution. In this work, we report the use of block copolymers (BCPs) as a solution to provide enhanced compatibility of the CNT in an epoxy-based matrix and as means to provide them further nanostructuration. Studied BCPs were especially formulated for epoxy matrices, being one of them customised to also have strong compatibility for CNT. BCPs were added to CNT without introduction of additional solvents. Different formulations were studied and the CNT dispersion, distribution and interaction with matrix were evaluated by rheology, electron microscopy and dynamic mechanical analysis. The results suggest that the customised BCP can have a significant improvement in the dispersion of the CNT, on the adhesion between the polymeric matrix and the CNT and can provide a mean for nanostructuration.

© 2018 Sociedade Portuguesa de Materiais (SPM). Published by Elsevier España, S.L.U. All rights reserved.

1. Introduction

Since their first discovery in 1991 by Iijima [1], carbon nanotubes (CNT) have received considerable attention due their multifunctional properties, with special emphasis on applications for reinforcement of high performance polymer composites [2]. For the specific application in carbon fibres reinforced polymer (CFRP) composites, CNT are usually introduced in thermosetting polymers, being epoxy matrices the most commonly explored [3].

However, due to strong attractive long-ranged Van der Waals interactions among the nanotubes, they tend to aggregate, being difficult achieve an homogeneous dispersion [4,5]. The quality of CNT dispersion, distribution and orientation in polymeric matrices is a determinant factor for the final properties of the composites and the limited capacity to control these parameters are often regarded as a limiting aspect for their application in composite formulations [6].

Currently used strategies for obtaining enhanced CNT dispersions in a polymeric matrix include the use of mechanical methods, covalent functionalisation and non-covalent modifications of the nanotubes [4,5], but the control of CNT distribution and alignment requires the combination of them. These methods can improve the compatibility with the polymeric matrix. However, typically covalent modifications can change the physical properties of the nanotubes, while mechanical methods only tend to stabilise the dispersion temporarily [7]. Non-covalent modifications, such as the use of surfactants, have been gaining relevance, once these methods improve the compatibility with the matrix without promoting changes in CNT structure [7–11]. Block copolymers (BCPs) are arrangements of two or more different blocks of polymers [12], and are considered highly stable surfactants for the dispersion of nanomaterials [13]. For the dispersion of CNT, BCPs are usually composed at least by one block that will be anchored to the CNT and one block with affinity to polymeric matrix [13,14]. Nanostrength BCPs (developed and supplied by Arkema) have a high potential for the formation of

* Corresponding authors.
E-mail addresses: jguedes@inegi.up.pt (J.F. Guedes), nrocha@inegi.up.pt (N. Rocha).

nanostructures in epoxy-based matrices due to their capability to self-assemble at nanometer scale [9,15].

Recently, BCPs have been reported as effective surfactants for CNT dispersions in epoxy resin matrices, improving at the same time mechanical properties by enhancing of interfacial adhesion between the nanotubes and the resin [7,10,16]. One disadvantage of the use of commercial BCPs is the absence of information about chemical structures of the polymeric blocks. For instance, the use of BCPs designed for pigment dispersion in polymeric matrices are expected to be poor anchoring block for CNT. This lack of information makes nearly impossible to establish correlations between their structure and performance. In fact, self-assembled BCPs nanostructures are widely dependent of the molecular design of the block copolymer and on the nature of the interactions between the dispersion medium, the component to be dispersed and the block copolymer (BCP). It is, therefore, expected that a suitable control of these parameters will allow obtaining composite formulations with enhanced processing and performance properties.

In the present work, it is studied the influence of using BCPs with different chemical natures, and, therefore, with different interactions with the CNT, in the dispersion of MWCNT in an epoxy matrix. The performance of a custom BCP, that have a block with higher affinity for CNT, is compared with other block copolymers with poly (butyl acrylate) (PBuA) combined with poly (methyl methacrylate) (PMMA) in normal form and hydrolysed, which are already commercially available to provide nanostructuration in epoxy-based polymeric matrices.

2. Materials and methods

2.1. Materials

An epoxy resin (LY556) with an anhydride curing agent (HY 906) and an imidazole catalyst (DY 070) were used as matrix system and were supplied by Hunstman.

The MWCNT were purchased in form of masterbatch pellets (Graphistrength, Arkema) with a concentration of 25 wt.% in LY556 and diluted in the same resin to obtain the final desired concentrations.

Nanostrength D51N, M51 and custom (C-BCP) block copolymers were used. All of them were supplied by Arkema and their characteristics are presented in Table 1.

2.2. Nanocomposites preparation

The most common approach used for preparation of nanocomposites with BCPs as dispersant of CNT, requires a

Table 2
Three-roll mill machine programme.

Cycle	Gap amplitude (μm)	Velocity (rpm)
1	80	200
2	60	200
3	40	150
4	20	150
5	10	100

Table 3
Nanocomposites prepared and their composition.

Sample designation	Components		
	Resin	CNT	BCP
ER	LY556	X	X
ER/CNT	LY556	1% CNT	X
ER/CNT/D51N	LY556	1% CNT	D51N
ER/CNT/M51	LY556	1% CNT	M51
ER/CNT/C-BCP	LY556	1% CNT	C-BCP

preliminary dissolution of BCPs in solvents [8–10,16]. However, for composite applications, it is important to ensure the total removal of solvent, since their residual presence decrease significantly the final performance of composite. In this work, it was used an approach where the BCPs were first dissolved in the resin, without the necessity of adding solvents.

Half of the resin required to obtain a final concentration of 1 wt.% was added to the CNT masterbatch. This mixture was mechanically stirred at 200 rpm during 10 min at 80 °C to decrease the viscosity and, thus, to promote dispersion. After this, the CNT mixture was dispersed in a three-roll mill machine in a programme with different velocities and gap amplitude (Table 2).

The BCP was added to the remaining amount of resin at the same loading as of CNT and placed in an ultrasonic bath for 15 min. Afterwards, the mixture of BCP and the resin was mechanically stirred at 200 rpm, during 10 min at 60 °C. Both mixtures were combined and dispersed in a three-roll mill with the same dispersion programme as previously described in Table 2. The hardener and catalyst were added and mechanically stirred at 200 rpm for 30 min at 60 °C. The mixture was then placed in an ultrasonic bath for 30 min to remove residual air and cured at 120 °C for 2 h and post-cured at 180 °C for 2 h.

Reference samples of resin, resin with different BCP and resin with CNT were also prepared using the same procedure. In Table 3 prepared nanocomposites are presented.

Table 1
Block copolymers studied and their characteristics.

Block copolymer	Type	Polymers	Affinity	
			Matrix	CNT
M51	Triblock	PMMA-b-PBuA-b-PMMA	√	×
D51N	Triblock	Hydrolysed PMMA-b-PBuA-b-PMMA	√	×
C-BCP	Diblock	PMMA and polymer with strong affinity for CNT	√	√

2.3. Nanocomposites characterisation

With purpose of achieving a complete evaluation of CNT dispersion and distribution, several characterisation techniques were combined and experimental conditions are described below. CNT/epoxy mixtures are known to behave non-Newtonian fluids [17,18] and, therefore, the dependency of viscosity of samples at different shear rates was evaluated using a Discovery HR-1 rheometer (TA instruments) with a 25 mm parallel plate aluminium geometry. A flow ramp method was performed at 30 °C with a range of shear rate between 0.085 and 1150 s^{-1}. These measurements were carried out on solutions before the addition of hardener and catalyst.

Transmission electron microscopy (TEM) carried out in a JEOL-JEM 1400 with an electron beam of 120 000 V. Nanocomposites specimens for TEM were obtained through an ultra-microtome.

Dynamic mechanical analysis (DMA) was performed using a Q800 DMA from TA Instruments. A temperature ramp with a heating rate of 2 °C/min from room temperature to 220 °C was performed with a frequency of 1 Hz in single cantilever mode.

Scanning electron microscopy (SEM) was performed using a FEI Quanta 400 FEG ESEM microscope. Nanocomposites were fractured in liquid nitrogen and covered with a layer of gold/palladium for increasing surface conductivity.

3. Results and discussion

3.1. Rheological behaviour

The study of viscosity variation at different shear rates was performed by rheological measurements and the obtained results are presented in Fig. 1. A detail of rheological behaviour of nanocomposites with BCPs are also shown to evaluate differences between the compositions.

ER presents a Newtonian behaviour, since viscosity is independent on the applied shear rate. The initial viscosity of ER is 4.5 Pa s and increase two orders of magnitude with the introduction of 1%wt. CNT. This behaviour is in agreement with previous studies [17–19]. The addition of BCP to ER/CNT did not change significantly the viscosity, which is seen as an important result, since the molecular weight of BCP could increase the mixture viscosity making the processing of formulations difficult. The small differences on epoxy/CNT mixtures indicate that the CNT have a more significant impact on viscosity than the

molecular weight of BCP. Samples with CNT present a shear thinning behaviour as obtained in other similar studies [17,18].

Although the order of magnitude in the viscosity is not changed, the detailed image indicates that the C-BCP and D51N increased viscosity when compared to ER/CNT, while M51 promoted a decrease of viscosity. Based on similar studies, higher viscosity means that dispersion is better [19] and, therefore, the results suggest that the C-BCP are promoting a better CNT dispersion, followed by D51N, while the BCP M51 is leading to a poor dispersion. However, it should be noted that these differences are small and that interface parameters can also affect significantly this property. Therefore, the dispersion was further evaluated through electron microscopy.

3.2. Carbon nanotubes distribution and dispersion

TEM analysis was carried out to evaluate dispersion and distribution of CNT and the obtained micrographs are shown in Fig. 2.

For the sample ER/CNT is observed that CNT are poorly distributed in analysed area, highlighting the presence of larger CNT agglomerates in two main areas (dashed line circle) and some small agglomerates (solid line circle).

Independently of their composition, the TEM micrographs suggest that the CNT are better dispersed when the BCPs are added. For nanocomposites ER/CNT/M51 and ER/CNT/C-BCP it can be observed that CNT are better dispersed and distributed in the analysed area, while ER/CNT/D51N still presented some agglomerates (red circle), but at the same time presents a good CNT distribution for analysed area. This result can indicate that the D51N BCP (due to more hydrophilic nature of some of the groups) have a poor dispersion capacity for the CNT than the other two BCPs.

Some white circular structures can be identified in the micrographs and more clearly at lower magnifications (Fig. 3). These nanostructures are visible for samples with BCPs and it is attributed to the formation of nanostructures without affinity to the CNT. Samples ER/CNT/M51 and ER/CNT/D51N present a greater number of these nanostructures, supporting the assumption that BCP with segments with poor affinity to the CNT are probably to form these independent structures. In the case of nanocomposite prepared with C-BCP this nanostructures are visualised in less number suggesting a better affinity for matrix and for the CNT.

3.3. Dynamic mechanical analysis

Storage modulus and tan δ variation with the temperature were obtained through dynamic mechanical analysis. Storage modulus profiles are presented in Fig. 4.

ER presents a storage modulus of 2654 MPa at nearly room temperature, being the nanocomposite with highest value. When CNT are added, storage modulus decreases to 2214 MPa, which can be attributed to deterioration of the matrix under flexing caused by defects during manufacturing. The addition of BCPs to ER/CNT increases slightly the storage modulus, being ER/CNT/M51 the nanocomposite with higher value of storage modulus. When compared to the ER, the reduction of storage
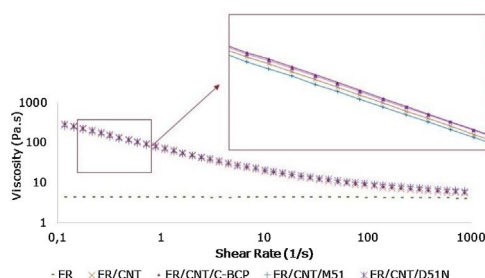

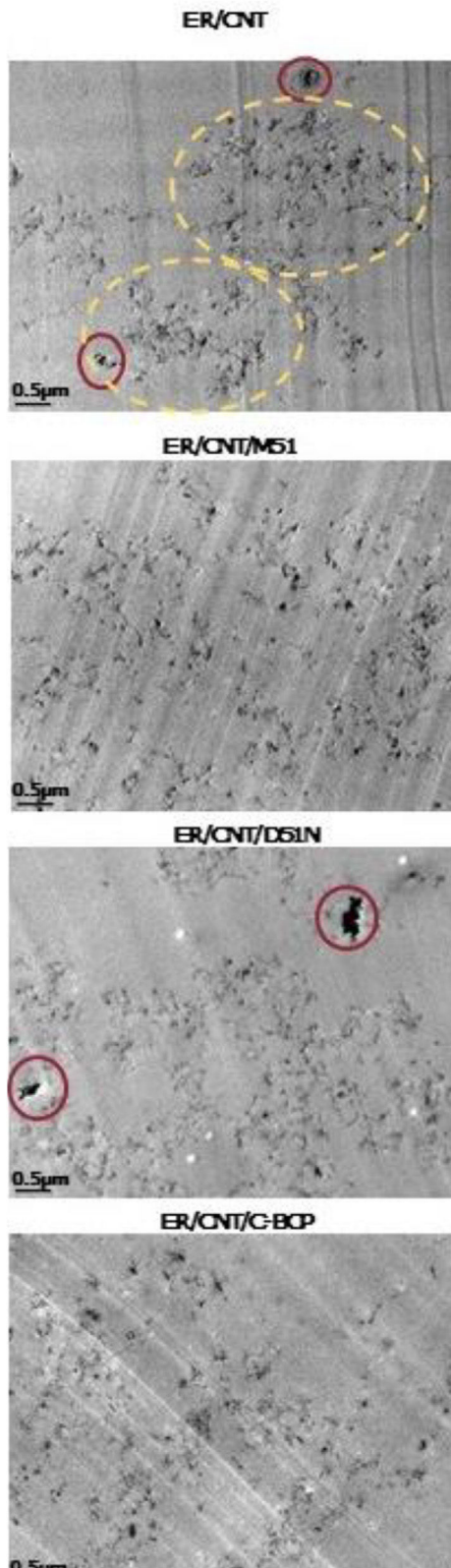Fig. 1. Viscosity variation at different shear rates.

ER/CNT

ER/CNT/M51

ER/CNT/D51N

ER/CNT/C-BCP

Fig. 2. TEM images of nanocomposites ER/CNT, ER/CNT/M51, ER/CNT/D51N and ER/CNT/C-BCP with a magnification of 25,000×.

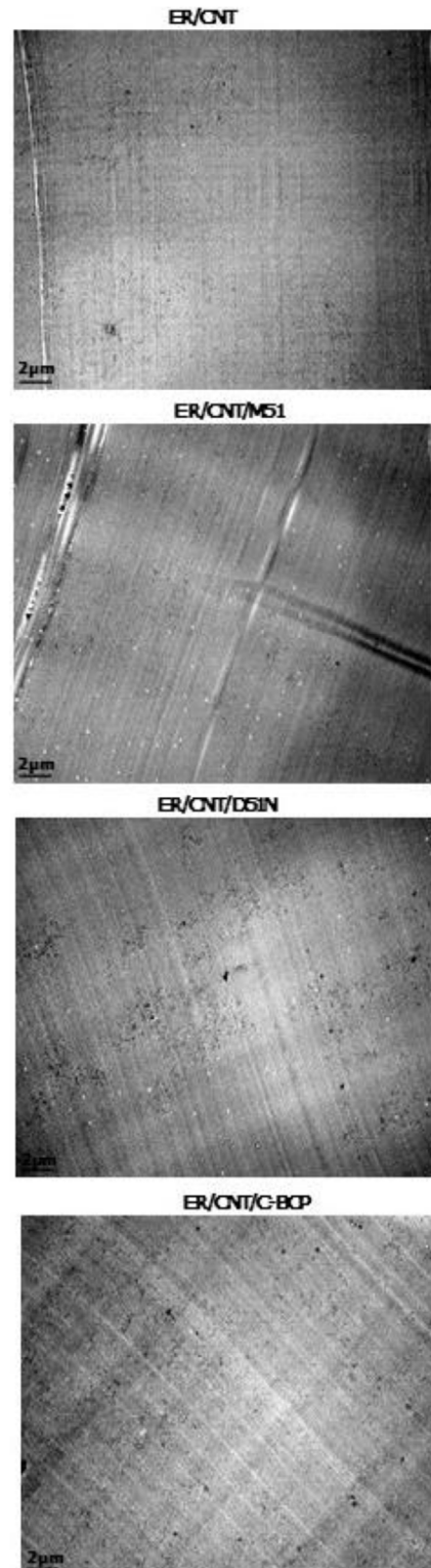**ER/CNT**

ER/CNT/M51

ER/CNT/D51N

ER/CNT/C-BCP

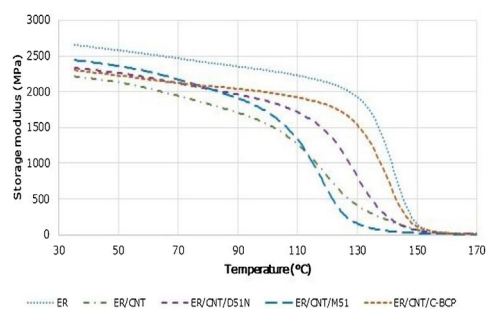Fig. 3. TEM images of nanocomposites ER/CNT, ER/CNT/M51, ER/CNT/D51N and ER/CNT/C-BCP with a magnification of 6000×.

Fig. 4. Storage modulus variation with temperature.

Table 4
Storage modulus and tan δ results in Tg region obtained by DMA analysis. Reduction of storage modulus is in function of ER at same temperature.

Sample designation	Storage modulus at (MPa)	Reduction of storage modulus in Tg zone (%)	Maximum tan δ peak (150 °C)
ER	2654	X	1.09
ER/CNT	2214	54.2	0.50
ER/CNT/M51	2442	85.1	0.46
ER/CNT/D51N	2331	59.6	0.67
ER/CNT/C-BCP	2298	23.4	0.92

Fig. 5. Fracture surface images of ER/CNT and ER/CNT/C-BCP with a magnification of 10,000×.

Fig. 6. Self-assembled nanostructures present in ER/CNT/C-BCP (magnification 50,000×).
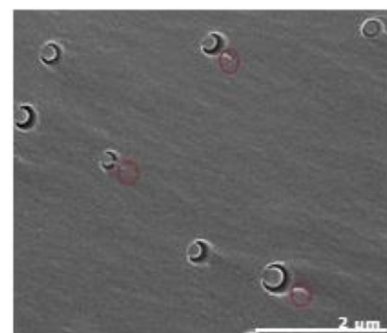
modulus can be attributed to the defects caused by the CNT but may also be attributed to the presence of a less brittle than the epoxy component (the BCP). In comparison to the sample filled only with CNT (ER/CNT), the increase in the storage modulus is due to an improvement of compatibility with the matrix [20]. Storage modulus reduction in Tg zone and Tan δ results are presented in Table 4.

3.4. Surface microstructure

SEM analysis allows to observe the microstructure of the fractured surface of the nanocomposites and the obtained micrographs are presented in Fig. 5.

ER/CNT presents a more prominent and rougher fracture surface. On the other hand, ER/CNT/C-BCP has a smoother fracture surface, suggesting that the BCPs not only improved the CNT distribution, but also improve the matrix toughness. This effect can be attributed to a better compatibility between CNT and matrix. Mechanical testing on these specimens is required to fully understand the effect of the BCPs in the nanocomposite formulation.

For samples with block copolymers, and similarly to what has been observed in TEM analysis, in SEM analysis is also observed the presence of regular spherical nanostructures (Fig. 6). Similar structures are reported in some studies with P(MMA-co-GMA) [21] or P(MMA-co-DMA)-b-(BA)-b-(MMA-co-DMA) [22] in epoxy matrices. Bashar *et al.* also observe the same structure type with M52 block copolymer (equivalent to M51 but with higher molecular weight) also in an epoxy matrix [23]. The presence of adjacent tail-like structures (marked in red) are present in these structures. Complementary studies are being performed to understand further the structure of these nanostructures and

to evaluate its impact on final nanocomposites mechanical and thermal properties.

4. Conclusions

The application of block copolymers in epoxy and CNT formulations is found to be a promising approach for CNT dispersion, providing at the same time the nanostructuration in epoxy matrices filled with CNT.

Nanocomposites prepared with C-BCP present better results comparatively to the others studied. The C-BCP was designed specifically to provide an improvement of compatibility with the CNT. This nanocomposite presents a viscosity in the same order of magnitude as epoxy/CNT mixtures without additional BCP. TEM micrographs suggest a better CNT distribution and an improvement of the affinity to the matrix, leading to a smoother

fracture. SEM micrographs also suggest that C-BCP can promote nanostructuration in epoxy-CNT formulations, but further studies are required to understand the mechanisms of nanostructuration, its final structure and the impact on performance properties of final composites.

Acknowledgements

References

[1] S. Iijima, Nature 354 (1991).
[2] O. Breuer, U. Sundararaj, Polym. Compos. 25 (2004) 630.
[3] J.N. Coleman, U. Khan, Y.K. Gun'ko, Adv. Mater. 18 (2006) 689.
[4] J. Zou, J. Liu, L. Zhai, Am. Chem. Soc. (2010) 95.
[5] P.-C. Ma, N.A. Siddiqui, G. Marom, J.-K. Kim, Compos. Part A: Appl. Sci. 41 (2010) 1345.
[6] X. Xie, Y. Mai, X. Zhou, Mater. Sci. Eng. R 49 (2005) 89.
[7] M.R. Loos, J. Yang, D.L. Feke, I. Manas-Zloczower, Compos. Sci. Technol. 72 (2012) 482.
[8] J. Cho, I.M. Daniel, Scripta Mater. 58 (2008) 533.
[9] A. Bajpai, A.K. Alapati, B. Wetzel, Proc. Struct. Integr. 2 (2016) 104.
[10] Q. Li, M. Zaiser, V. Koutsos, Phys. Status Solidi A 201 (2004) R89.
[11] L.H. Esposito, J.A. Ramos, G. Kortaberria, Prog. Org. Coat. 77 (2014) 1452.
[12] G. Riess, Prog. Polym. Sci. 28 (2003) 1107.
[13] J.K. Kim, S.Y. Yang, Y. Lee, Y. Kim, Prog. Polym. Sci. 35 (2010) 1325.
[14] A.-V. Ruzette, L. Leibler, Nature Mater. 4 (2005) 19.
[15] P. Arkema Inc., France, www.nanostrength.com2013.
[16] Q. Li, M. Zaiser, J.R. Blackford, C. Jeffree, Y. He, V. Koutsos, Mater. Lett. 125 (2014) 116.
[17] A. Allaoui, N. Bounia, Curr. Nanosci. 6 (2010) 158.
[18] R. Nadiv, G. Vasilyev, M. Shtein, A. Peled, E. Zussman, O. Regev, Compos. Sci. Technol. 133 (2016) 192.
[19] G.V. Ramana, B. Padya, R.N. Kumar, K.V.P. Prabhakar, P.K. Jain, IJEMS 17 (2010).
[20] M. Naebe, J. Wang, A. Amini, H. Khayyam, N. Hameed, L.H. Li, Y. Chen, B. Fox, Sci. Rep. 4 (2014) 4375.
[21] J.M. Dean, R.B. Grubbs, W. Saad, R.F. Cook, F.S. Bates, J. Polym. Sci. Pol. Phys. 41 (2003).
[22] S. Maiez-Tribut, J.P. Pascault, J. Borrajo, J.J. Williams, Macromolecules 40 (2007).
[23] M.T. Bashar, U. Sundararaj, P. Mertiny, Polym. Eng. Sci. 54 (2014) 1047.